



## UvA-DARE (Digital Academic Repository)

### An atom interferometer enabled by spontaneous decay

Cornelussen, R.A.; Spreeuw, R.J.C.; van Linden van den Heuvell, H.B.

**Publication date**  
2005

**Published in**  
Physical Review A

[Link to publication](#)

#### **Citation for published version (APA):**

Cornelussen, R. A., Spreeuw, R. J. C., & van Linden van den Heuvell, H. B. (2005). An atom interferometer enabled by spontaneous decay. *Physical Review A*, 71, 033627.

#### **General rights**

It is not permitted to download or to forward/distribute the text or part of it without the consent of the author(s) and/or copyright holder(s), other than for strictly personal, individual use, unless the work is under an open content license (like Creative Commons).

#### **Disclaimer/Complaints regulations**

If you believe that digital publication of certain material infringes any of your rights or (privacy) interests, please let the Library know, stating your reasons. In case of a legitimate complaint, the Library will make the material inaccessible and/or remove it from the website. Please Ask the Library: <https://uba.uva.nl/en/contact>, or a letter to: Library of the University of Amsterdam, Secretariat, Singel 425, 1012 WP Amsterdam, The Netherlands. You will be contacted as soon as possible.

## An atom interferometer enabled by spontaneous decay

R. A. Cornelussen, R. J. C. Spreeuw, and H. B. van Linden van den Heuvell\*

*Van der Waals–Zeeman Institute, University of Amsterdam, Valckenierstraat 65, 1018 XE Amsterdam, The Netherlands*

(Received 15 November 2004; published 25 March 2005)

We investigate the question as to whether Michelson-type interferometry is possible if the role of the beam splitter is played by a spontaneous process. This question arises from an inspection of trajectories of atoms bouncing inelastically from an evanescent-wave (EW) mirror. Each final velocity can be reached via two possible paths, with a *spontaneous* Raman transition occurring during either the ingoing or the outgoing part of the trajectory. At first sight, one might expect that the spontaneous character of the Raman transfer would destroy the coherence and thus the interference. We investigated this problem by numerically solving the Schrödinger equation and applying a Monte Carlo wave-function approach. We find interference fringes in velocity space, even when random photon recoils are taken into account.

DOI: 10.1103/PhysRevA.71.033627

PACS number(s): 03.75.Dg, 03.65.Yz, 39.20.+q

### I. INTRODUCTION

Spontaneous emission is generally considered a detrimental effect in atom interferometers. The associated random recoil reduces or even completely destroys the visibility of the interference fringes. In this paper, we describe an atom interferometer where the beam splitter works by means of a spontaneous Raman transition. Our central question will be whether one can observe interference in such an interferometer which is enabled by a spontaneous process and where decoherence is built into the beam splitting process from the start.

The role of spontaneous emission in (atom) interferometers has long been connected to the concept of which-way information, ultimately tracing back to Heisenberg's uncertainty principle [1]. Feynman [2] discussed a *Gedankenexperiment* using a Heisenberg microscope to determine which slit was taken by a particle in a Young's two-slit interferometer. The scattered photon, needed to determine the position, spoils the interference pattern due to its associated recoil. Similarly, spontaneous emission in an (atom) interferometer may provide position information on the atom, while at the same time randomizing the momentum and spoiling interference [3,4]. On the other hand, resonance fluorescence, including that from spontaneous Raman transitions, is as coherent as the incident light in the limit of low saturation [5,6]. Experimental demonstrations have been given by Eichmann *et al.* [7] and Cline *et al.* [8]. An experiment by Dürr *et al.* [9] has made it clear that the availability of which-way information should be conceptually separated from the presence of random recoils. Which-way information can be obtained without random recoils, nevertheless leading to a loss of interference. Here, we show that random recoils do not lead to a loss of interference as long as the spontaneously emitted photons do not yield which-way information.

Our proposed interferometer is based on cold atoms that reflect from an evanescent-wave (EW) mirror. Our model atom is a typical alkali atom with two hyperfine ground

states. During the reflection from the EW mirror, the atoms can make a spontaneous Raman transition to the other hyperfine state. When the repulsive potential experienced by the final state is lower, the atoms lose kinetic energy and hence bounce inelastically from the potential [10,11]. This Sisyphus process has been investigated previously [12] and the resulting final velocity distribution has been shown to be a caustic [13], reminiscent of the rainbow. Furthermore it is used in several experiments as the loading process of (low-dimensional) traps for atoms [14–16]. Cagnet *et al.* [17] observed the analog of Stückelberg oscillations in the transverse velocity distribution of atoms that reflect elastically from a corrugated EW potential. However, no stochastic or incoherent processes were involved.

In our case, the final velocity of an atom depends on the position where it made the Raman transfer [13]. Looking at the trajectories in detail, we see that each final velocity can be reached by two trajectories, as is shown in Fig. 1. An atom can be transferred to the second state on the ingoing or the outgoing part of its trajectory. Interference will manifest itself in the velocity distribution of the reflected atoms, since the outgoing velocity depends on the transition point  $z$ . Note that the beam splitter, its role being played by a spontaneous Raman transition, is highly nonunitary: Atoms are only transferred from state  $|1\rangle$  to state  $|2\rangle$  and not vice versa.

This paper is structured as follows. We first present a semiclassical picture, and use it to make qualitative predic-

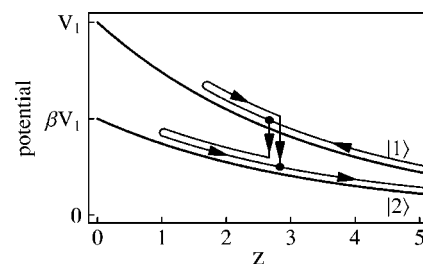


FIG. 1. Atoms approaching an EW mirror in state  $|1\rangle$  can undergo a spontaneous transition to state  $|2\rangle$ , on either the ingoing or the outgoing part of the trajectory. These two paths possibly interfere with a phase difference depending on the transition point  $z$ .

\*Email address: heuvell@science.uva.nl

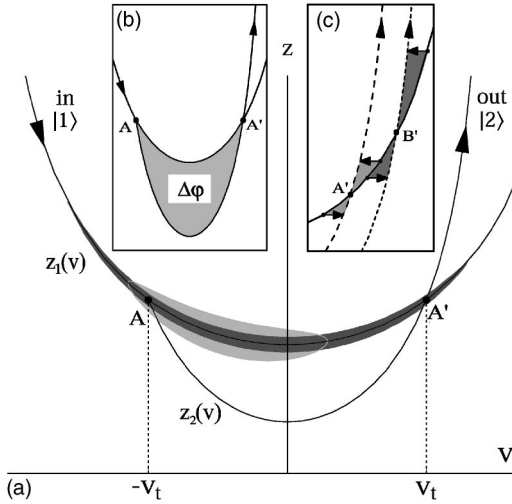


FIG. 2. Phase-space trajectories of atoms being repelled by an evanescent potential. Atoms initially in state  $|1\rangle$  can be transferred to state  $|2\rangle$  and continue on a different path through phase space. (a) Depending on the initial shape of the wave packet (e.g., the light and dark gray areas) which-way information can be obtained or not. (b) The accumulated phase difference between these two paths, indicated by the enclosed gray area, may give rise to interference effects. (c) A momentum kick due to the spontaneous recoil gives rise to an extra phase contribution.

tions about the behavior of the interference effects, if present. The question as to whether interference is possible will be answered by solving the Schrödinger equation in two different ways. The first approach will employ stationary analytical solutions of the time-independent Schrödinger equation, but is limited to monochromatic wave functions. The second approach will propagate a wave packet by numerically integrating the time-dependent Schrödinger equation with random quantum jumps describing the Raman transitions. The last section deals with experimental considerations.

## II. SEMICLASSICAL DESCRIPTION

The analysis will be for a two-level atom, and only the motion of the atom in the direction along the EW-potential gradient will be considered. The calculations throughout this paper will assume a low saturation parameter, so that depletion of the initial state can be neglected. An atom in state  $|1\rangle$  that reflects from an EW mirror experiences a potential  $V_1 \exp(-2\kappa z)$ , with  $\kappa^{-1}$  as the decay length of the EW field. The atom's trajectory through phase space is given by  $z_1(v) = (-1/2\kappa) \ln[(m/2V_1)(v_i^2 - v^2)]$ , with  $v_i$  as the velocity with which the atom enters the potential, see Fig. 2. After a transition to state  $|2\rangle$  in point A or A', the atom experiences a potential  $\beta V_1 \exp(-2\kappa z)$ , with  $\beta < 1$  as the factor by which the potential energy is reduced after the Raman transition. The atom continues its way through phase space on a new trajectory  $z_2(v)$ , given by  $z_2(v) = (-1/2\kappa) \ln[(m/2\beta V_1)(v_f^2 - v^2)]$ , with  $v_f$  as the asymptotic velocity with which the atom leaves the potential. The final velocity can have any value between  $v_f = \sqrt{\beta}v_i$ , which corresponds to a transfer in

the turning point, and  $v_f = v_i$ , which corresponds to a transfer outside the EW potential. The final velocity depends on the atom's velocity  $v_t$  at the moment of the transfer to state  $|2\rangle$ . This dependence is given by  $v_f^2 = v_t^2 + \beta(v_i^2 - v_t^2)$ , from which it is clear that two values  $\pm v_t$  lead to the same final velocity  $v_f$ . The two transitions lead to two possible trajectories through phase space, as shown in Fig. 2(a). The phase difference  $\Delta\phi$  between the two trajectories is given by

$$\Delta\phi = \frac{m}{\hbar} \int_{-v_t}^{v_t} [z_1(v) - z_2(v)] dv. \quad (1)$$

This phase difference is proportional to the area between the two curves, indicated in gray in Fig. 2(b). From the evaluation of the integral for various parameters, we learn that the fringe period decreases for increasing initial velocities  $v_i$ , for increasing final velocities  $v_f$ , for smaller  $\beta$  and for larger decay length (smaller  $\kappa$ ).

In a semiclassical picture, the atom can be treated as a wave packet which is subject to Heisenberg's uncertainty relation  $\Delta z \Delta v_z \geq \hbar/2m$ . The distribution of uncertainty between position  $z$  and momentum  $mv_z$  is determined by the experimental preparation procedure of the atoms. For a wave packet that initially has a large spread in momentum, it is not possible to unambiguously determine the phase difference between the two possible paths, since the wave packet is spread out over several classical trajectories through phase space. This is indicated by the light gray area in Fig. 2(a). It is, however, possible to determine whether the transfer to state  $|2\rangle$  is on the ingoing or outgoing path, by observing the timing of the spontaneously emitted photon. Therefore, it is not expected that wave packets with this shape show interference. On the other hand, a minimum uncertainty wave packet with a narrow initial momentum spread will more closely follow a classical trajectory through phase space. This is indicated by the dark gray area in Fig. 2(a). The phase difference between the two paths is well defined. The two points in phase space, A and A', where a transition to the final trajectory is possible, are covered simultaneously by the wave packet. Thus, no which-way information can be obtained by observing the time of emission of the spontaneously emitted photon. The initial trade-off between position and momentum uncertainty in a bandwidth-limited wave packet determines whether or not interference can be *a priori* excluded.

The random direction of the spontaneously emitted photon can be taken into account in the motion of the atom by a random momentum jump. This makes the atom propagate on a different trajectory through phase space than it would have without the random recoil. The momentum changes are indicated by horizontal arrows in the phase-space diagram of Fig. 2(c). For a single atom, or a collection of distinguishable atoms, the spontaneous recoil could be measured by detecting the direction in which the photon was emitted. Due to this possibility there will be a set of interference patterns, one for each recoil direction. By disregarding the information present in the scattered photons, we probe the incoherent sum of all these interference patterns. The phase difference between the two paths is different with respect to the recoil

free case, and it depends on the direction of the recoil. It is indicated by the gray areas in Fig. 2(c). In order for the interference to be experimentally observable, the difference between the interference patterns with a certain recoil direction should not be too large. This means that the phase difference between recoil components in the  $\pm z$  directions should be less than  $\pi$ . For larger final velocities, these phase corrections get larger as is apparent from comparing the areas around the point B' with the areas around point A' in Fig. 2(c). We thus expect the visibility of the interference to decrease for larger final velocities.

Note that which-way information cannot be retrieved from a measurement of the frequency  $\omega$  of the emitted photon. This frequency is determined by energy conservation:  $\hbar\omega = (1/2)m(v_i^2 - v_f^2) + \hbar\omega_{\text{EW}} - \hbar\Delta_{12}$ , where  $\omega_{\text{EW}}$  is the frequency of the evanescent photon and  $\hbar\Delta_{12}$  is the energy difference between states  $|1\rangle$  and  $|2\rangle$ . Because the initial and final kinetic energies are equal for both trajectories, the frequency of the spontaneously emitted photon is equal for both interfering paths.

### III. TIME-INDEPENDENT APPROACH

The question as to whether interference is visible will be answered in this section by considering analytical solutions of the time-independent Schrödinger equation

$$-\frac{\hbar^2}{2m}\frac{\partial^2}{\partial z^2}\psi_1(z) + V_1 e^{-2\kappa z}\psi_1(z) = \frac{p_0^2}{2m}\psi_1(z), \quad (2)$$

describing stationary states with a total energy  $p_0^2/2m$  on the potential  $V_1 \exp(-2\kappa z)$ . It thus describes particles with momentum  $\pm p_0$  in the asymptotic limit of large  $z$ . This is one of the few examples where the eigenfunctions of the Schrödinger equation are known analytically. The solutions are given by

$$\psi_1(z) = \sqrt{\frac{4p_0}{\pi\hbar\kappa}} \sinh\left(\frac{\pi p_0}{\hbar\kappa}\right) K_{ip_0/\hbar\kappa}\left(\frac{\sqrt{2mV_1}}{\hbar\kappa} e^{-\kappa z}\right), \quad (3)$$

where  $K_\alpha(\cdot)$  is the Bessel-K function of order  $\alpha$  [18]. These functions are normalized such that the asymptotic density is independent of  $p_0$ . They are also given by [19] where a different normalization is used.

This wave function describes the atoms that are incident in state  $|1\rangle$ . After the spontaneous Raman transition to state  $|2\rangle$ , the atoms are described by one of the eigenfunctions  $\psi_{2,p}(z)$  with final momentum  $p$  in the potential  $V_2 \exp(-2\kappa z)$ . The final wave function in momentum space is given by the overlap integral

$$\phi_k(p) \propto \int_{-\infty}^{\infty} \psi_1(z) e^{-\kappa z - ikz} \psi_{2,p}^*(z) dz, \quad (4)$$

where the recoil due to the absorbed evanescent photon is taken into account by the factor  $\exp(-\kappa z)$  and the recoil due to the spontaneously emitted photon by the factor  $\exp(-ikz)$ , with  $\hbar k$  as the momentum component of the recoil in the  $z$  direction. As already discussed, there will be interference patterns  $|\phi_k(p)|^2$  for every value  $\hbar k$  of the recoil. A measurement that disregards the emitted photon yields the

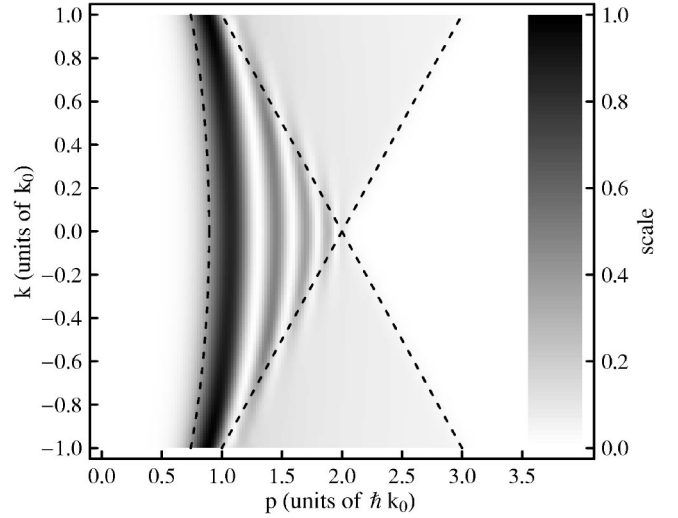


FIG. 3. The behavior of the interference pattern  $|\phi_k(p)|^2$  versus the final momentum  $p$ , expressed in units of the photon recoil  $\hbar k_0$ , for various values of the  $z$  component of the photon recoil  $\hbar k$  for parameters  $p_0 = 2\hbar k_0$ ,  $\kappa = k_0/8$ , and  $\beta = 0.2$ . The dashed curve indicates the classically lowest reachable momentum. Interference is visible in the area that can be reached by two trajectories, enclosed by the dashed curve and straight lines. The triangular regions can only be reached by one trajectory and hence no interference is visible.

sum of all these possible interference patterns. In this derivation, we will assume an isotropic distribution of the recoil momentum  $\hbar k$ . This is an approximation, since the distribution depends on the polarization of the spontaneously emitted photon. We will come back to this point in Sec. V. This leads to

$$|\phi(p)|^2 = \int_{-k_0}^{+k_0} |\phi_k(p)|^2 dk, \quad (5)$$

with  $\hbar k_0$  the total recoil momentum.

Figure 3 shows the behavior of the momentum distribution for various values of the  $z$  component of the photon recoil  $\hbar k$ . It is calculated using Eq. (4), with an initial momentum  $p_0 = 2\hbar k_0$ , a potential steepness  $\kappa = k_0/8$ , and potential reduction  $\beta = 0.2$ . The main features of this figure can be understood from semiclassical arguments.

The dashed curved and straight lines demarcate three separate classically allowed regions, taking into account the recoil. The dashed curve on the left indicates the lowest classically reachable momentum, given by  $p = \sqrt{\beta p_0} \sqrt{1 - (\hbar k/p_0)^2 / (1 - \beta)}$ . To the right of this curve, we clearly see a region with interference. In addition, we see two triangular regions with no interference, demarcated by two straight lines described by  $p = p_0 \pm \hbar k$ . The triangular regions can be reached by a single phase-space trajectory only. The upper (lower) triangle corresponds to a trajectory where the Raman transfer took place on the outgoing (incoming) branch. Only the region on the left of the triangles is reachable by two trajectories and thus shows interference.

The left dashed curve is reached by atoms that scatter a photon near the turning point. Note that in this case the pho-

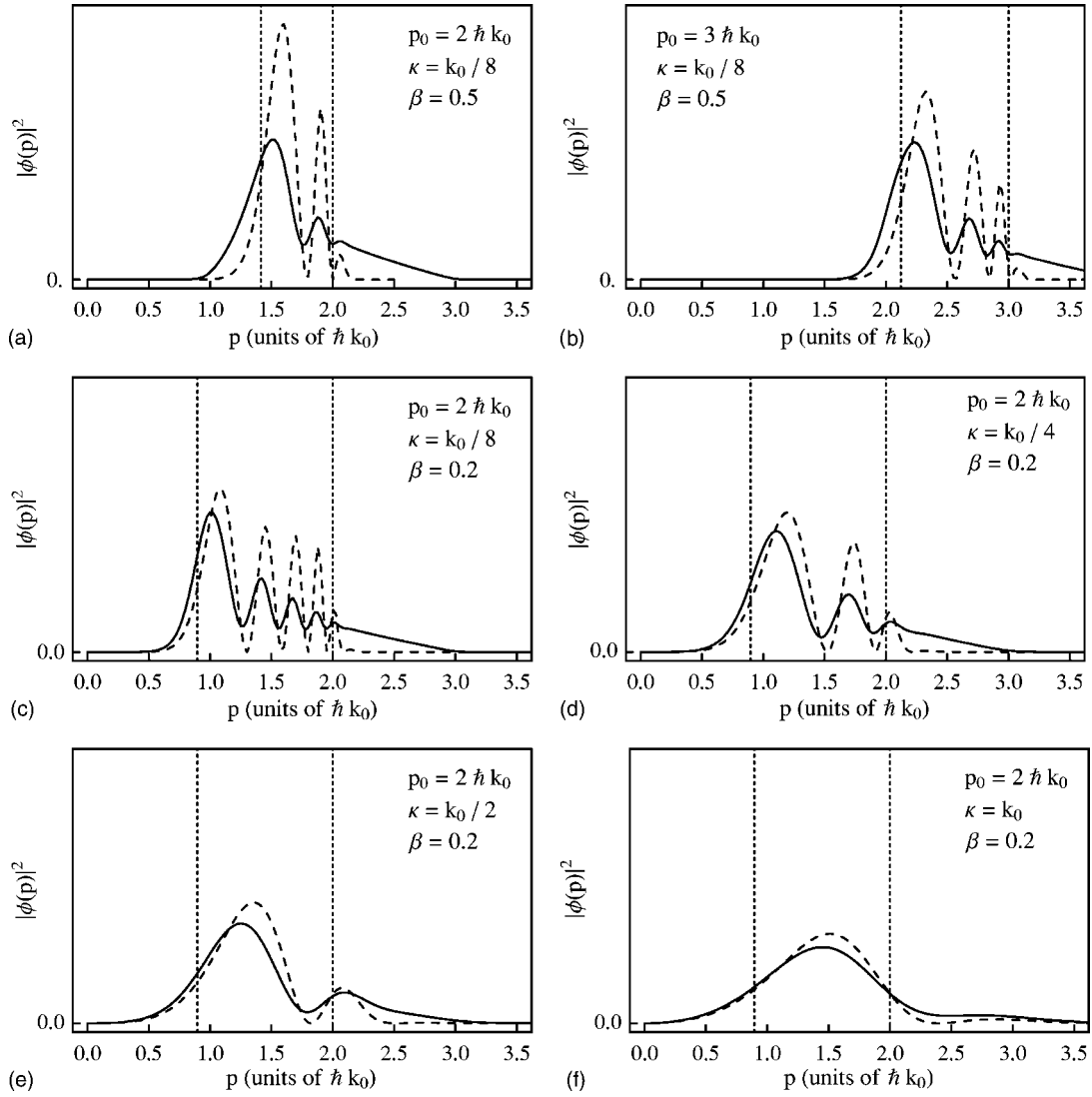


FIG. 4. Final momentum distributions  $|\phi(p)|^2$  calculated for different parameters using the time-independent method. Solid lines including the effect of a spontaneous recoil, and dashed lines without the effect of recoils, versus the final momentum  $p$  in units of the photon recoil  $\hbar k_0$ . The dotted lines indicate the classically allowed region without recoil. Between (a) and (b) the initial momentum  $p_0$  is changed, (a) and (c) differ in the reduction factor  $\beta$ , and (c)–(f) are a sequence for decreasing decay length  $\kappa^{-1}$ .

ton recoil has only a small influence on the final momentum  $p$ . The final momentum is mainly determined by the potential energy near the turning point that is converted to kinetic energy. The amount of kinetic energy that can be added or removed by the photon recoil near the turning point is small because the atomic velocity is small. As a result, we see only a slight curvature as a function of the recoil  $k$ . For larger values of the initial momentum  $p_0$  or the ratio  $\beta = V_2/V_1$ , the left curve will become straighter.

As expected, the main part of the momentum distribution is in the classically allowed regions. The distributions peak near the lower classical limit (the dashed curve), resembling the caustic distribution [13]. For every recoil direction, interference is visible. Although the region with interference is smaller for larger values of the recoil, the remaining interference fringes are present at more or less the same final momenta. This indicates that the spontaneous recoil does not completely wash out the interference. The behavior of the

interference does not depend on the sign of the recoil, because a photon that is emitted on the ingoing part of the trajectory has the same effect on the momentum distribution as a photon that is emitted in the opposite direction on the outgoing part of the trajectory.

Figure 4 shows the final momentum distribution, calculated by Eq. (5) for various experimental parameters. The results are compared with an evaluation without a stochastic contribution. Indeed, the averaging over the spontaneous recoil does not destroy the interference pattern. The small part of the distribution that extends into the classically forbidden region is an evanescent matter wave. Several of our predictions that were made for the general case of a coherent interferometer are noticeable in these graphs. Indeed, the fringe spacing decreases for larger initial and final momenta, for longer decay lengths  $\kappa^{-1}$  of the evanescent field, and for smaller values of  $\beta$ . Furthermore, as predicted for the case of an incoherent interferometer, the visibility of the graphs in

which the effect of the recoil has been taken into account decreases for larger final momenta.

#### IV. TIME-DEPENDENT APPROACH

In the previous section, we have shown that the incoherent nature of the spontaneous Raman transfer does not prevent us from observing interference. In this section, we show that the interference phenomena will also be visible for a wave packet with a finite momentum spread. In the analysis, we closely follow the Monte Carlo wave-function approach [20,21].

We consider the evolution of a diffraction-limited wave packet in state  $|1\rangle$

$$\psi_1(z, t=0) = \sqrt{\frac{1}{(2\pi)^{1/2}\sigma_z}} e^{ik_z z} e^{-(z-z_0)^2/4\sigma_z^2}, \quad (6)$$

with initial height  $z_0$ , initial width  $\sigma_z$ , and initial momentum  $p_0 = \hbar k_z$ . It is normalized such that  $\int |\psi(z, 0)|^2 dz = 1$  and  $\int (z - z_0)^2 |\psi(z, 0)|^2 dz = \sigma_z^2$ . The evolution of the wave packet when it reflects from the EW potential with a potential height  $V_1$  at  $z=0$  is calculated by numerically solving the time-dependent Schrödinger equation

$$i\hbar \frac{\partial}{\partial t} \psi_1(z, t) = -\frac{\hbar^2}{2m} \frac{\partial^2}{\partial z^2} \psi_1(z, t) + V_1 e^{-2\kappa z} \psi_1(z, t), \quad (7)$$

using the *Quantum kernel* [22] package in MATHEMATICA [23]. This results in a wave packet  $\psi_1(z, t)$  at time  $t$ . At a time  $\tau$ , a spontaneous Raman transition to state  $|2\rangle$  occurs, and the evolution abruptly continues on a potential that is a factor  $\beta$  lower. Immediately after the transfer, the wave function in state  $|2\rangle$  is described by

$$\psi_{\tau,k}(z, t = \tau) = \mathcal{N} \psi_1(z, \tau) e^{-\kappa z} e^{-ikz}, \quad (8)$$

where  $\mathcal{N}$  denotes a normalization factor. The two exponents are equal to the exponents in Eq. (4). The evolution of this wave function can now be continued up to a time  $t_{\text{end}}$ , leading to a wave function  $\psi_{\tau,k}(z, t_{\text{end}})$ . When  $t_{\text{end}}$  is large enough, the entire wave packet effectively propagates in free space, so that the momentum distribution remains constant. The Fourier transform

$$\phi_{\tau,k}(p) = \mathcal{F}[\psi_{\tau,k}(z, t_{\text{end}})] \quad (9)$$

of the wave packet at this time is the wave function in momentum space that endured a momentum kick  $\hbar k$  at its transfer time  $\tau$ . The transfer rate  $\Gamma(\tau)$  at a certain time  $\tau$  is given by

$$\Gamma(\tau) \propto \int_0^\infty \psi_1^*(z, \tau) V_1(z) \psi_1(z, \tau) dz. \quad (10)$$

We again assume an isotropic distribution of the recoil momentum  $\hbar k$ . Contributions with different  $\tau$  and  $k$  have to be summed in an incoherent way. For the momentum distribution as a function of the wave vector of the spontaneously emitted photon, we get

$$|\phi_k(p)|^2 \propto \int_0^{t_{\text{end}}} \Gamma(\tau) |\phi_{\tau,k}(p)|^2 d\tau. \quad (11)$$

A subsequent integration over this wave vector yields

$$|\phi(p)|^2 = \int_{-k_0}^{k_0} |\phi_k(p)|^2 dk \quad (12)$$

for the momentum distribution of a sample of atoms.

Figure 5 shows graphs of  $|\phi(p)|^2$  for some parameters. All calculations are performed with  $t_{\text{end}} = 70m/\hbar k_0^2$  for which the criterium that the entire wave packet has left the potential is fulfilled. Figure 5(a) should be compared with Fig. 4(a). The parameters for Figs. 5(b)–5(d) are equal to the parameters used for Fig. 4(c) except for the initial width  $\sigma_z$  of the wave packet and thus the momentum spread  $\sigma_p = \hbar/\sigma_z$ . Also for a wave packet with a finite momentum spread, the interference effects are present. As expected, the interference fringes are more apparent for a wave packet with a smaller momentum spread.

#### V. EXPERIMENTAL CONSIDERATIONS

So far, we have considered levels  $|1\rangle$  and  $|2\rangle$  without discussing to which physical level they correspond. In reality we usually deal with multilevel atoms, that moreover include substructure. Each of these (sub-)levels has a different interaction with the evanescent field. If more (sub-)levels contribute to the signal, the predicted interference can be washed out. For  $^{87}\text{Rb}$  atoms, a convenient choice would be the  $|Fm\rangle = |1, 0\rangle$  ground state for state  $|1\rangle$  and the  $|Fm\rangle = |2, \pm 1\rangle$  ground states for state  $|2\rangle$ . The evanescent field needs to be linearly ( $\pi$ ) polarized and blue detuned with respect to the  $F=1 \rightarrow F'=2$  transition of either the  $D_1$  or  $D_2$  line. Due to selection rules, only a transition over the  $|F'm'\rangle = |2, 0\rangle$  excited state contributes to the transition from state  $|1\rangle$  to state  $|2\rangle$ . This excited state can decay to either of the  $|2, \pm 1\rangle$  ground states by emitting a  $\sigma^\pm$  polarized photon. Since these states interact identically with the evanescent field, their interference patterns will overlap.

The necessary linear polarization for the EW can only be easily obtained using a transverse electric (TE) ( $\perp z$ ) polarized incident beam. For a circularly polarized photon, the distribution of wave vectors of the spontaneously emitted photon is nonisotropic. The circularly polarized photon has its quantization axis along the polarization axis of the EW field. The recoil distribution in the  $z$  direction due to such a photon is given by  $(3/16)[3 - (k/k_0)^2]$ . Intensity distributions of dipole radiation are given by, e.g., [24]. Since this distribution has a maximum for  $k=0$ , for which the recoil-dependent interference patterns are most pronounced as is visible in Fig. 3, the visibility of the interference signals will be slightly better than presented in this paper.

#### VI. DISCUSSION AND CONCLUSIONS

The calculations presented in this paper have been performed for low initial velocities  $v_i$ . This is because both calculation procedures turned out to be limited by computa-

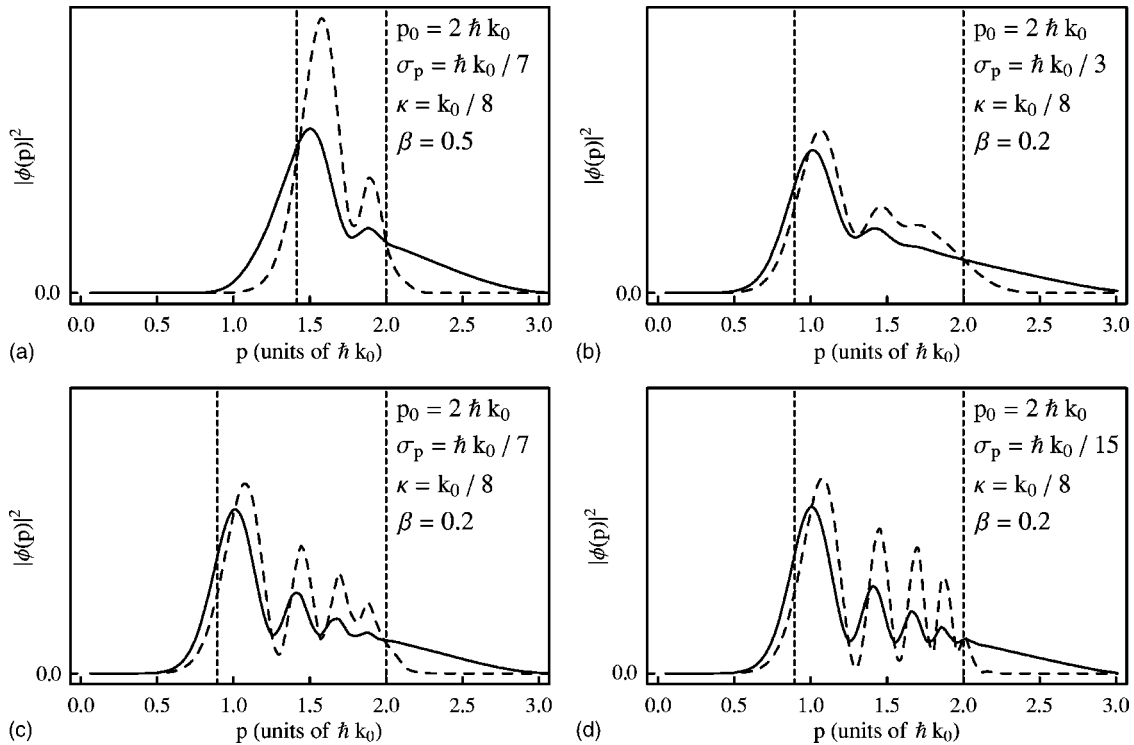


FIG. 5. Interference patterns calculated for different parameters calculated using the time-dependent method. Solid lines:  $|\phi(p)|^2$ , with the effect of a spontaneous recoil, and dashed lines:  $|\phi_0(p)|^2$ , without the effect of a spontaneous recoil, versus the final momentum  $p$  in units of the photon recoil  $\hbar k_0$ . The dotted lines indicate the classically allowed region without recoil. Between (a) and (c) the reduction factor  $\beta$  is changed, and (b)–(d) are a sequence where the initial momentum spread  $\sigma_p$  is decreased.

tional resources. For the time-independent approach the evaluation in MATHEMATICA [23] of the Bessel-K functions of high imaginary order becomes very slow. For the time-dependent approach, the number of sampling points, necessary for the numerical evaluation, becomes too large due to the highly oscillatory character of the incident wave packet. However, we expect even better signals for realistic values for the initial velocity  $v_i$ , so the calculation represents a worst case.

By numerically solving the Schrödinger equation, we can now reply with an unambiguous yes to the question, “*can the beam splitter in an atom interferometer work on the basis of spontaneous emission?*” The intuitive objections to whether this is possible have been refuted. The semiclassical arguments have been confirmed by the full quantum-mechanical calculations. Which-way information due to the possibility of detecting the time of emission of the spontaneously emitted photon is avoided by choosing a sufficiently narrow velocity uncertainty. A wave packet covers both transfer points in phase space simultaneously if its velocity is defined accurately enough. The incoherent nature of a spontaneous emis-

sion process due to the random recoil direction of the atom is visible in all the calculated interference curves, but does not lead to a complete scrambling of the interference. For larger final velocities, for which the transfer points are separated more and the acquired random phase is consequently larger, the visibility of the interference fringes indeed decreases. Furthermore the fringe period indeed qualitatively shows the behavior that was predicted on the basis of the semiclassical calculations.

Our analysis also shows that the absence or presence of which-way information is not the same as the perturbing effect of the recoils due to spontaneous transitions. This is most clearly seen in Fig. 2 and is in agreement with the viewpoint of Dürr *et al.* [9].

#### ACKNOWLEDGMENTS

This work is part of the research program of the “Stichting voor Fundamenteel Onderzoek van de Materie” (FOM) which is financially supported by the “Nederlandse Organisatie voor Wetenschappelijk Onderzoek” (NWO).

[1] W. Heisenberg, *Z. Phys.* **43**, 172 (1927).

[2] R. P. Feynman, R. B. Leighton, and M. Sands, *Lectures on Physics* (Addison-Wesley, Reading, MA, 1965), Vol. 3.

[3] M. S. Chapman, T. D. Hammond, A. Lenef, J. Schmiedmayer,

R. A. Rubenstein, E. Smith, and D. E. Pritchard, *Phys. Rev. Lett.* **75**, 3783 (1995).

[4] L. Hackermüller, K. Hornberger, B. Brezger, A. Zeilinger, and M. Arndt, *Nature (London)* **427**, 711 (2004).

- [5] R. Loudon, *The Quantum Theory of Light*, 2nd ed. (Clarendon, Oxford, 1983).
- [6] C. Cohen-Tannoudji, J. Dupont-Roc, and G. Grynberg, *Atom Photon Interactions* (Wiley Interscience, New York, 1998).
- [7] U. Eichmann, J. C. Bergquist, J. J. Bollinger, J. M. Gilligan, W. M. Itano, D. J. Wineland, and M. G. Raizen, *Phys. Rev. Lett.* **70**, 2359 (1993).
- [8] R. A. Cline, J. D. Miller, M. R. Matthews, and D. J. Heinzen, *Opt. Lett.* **19**, 207 (1994).
- [9] S. Dürr, T. Nonn, and G. Rempe, *Nature (London)* **395**, 33 (1998).
- [10] K. Helmerson, S. Rolston, L. Goldner, and W. Phillips, Workshop on Optics and Interferometry with Atoms, Insel Reichenau, Germany, June 1992 (unpublished); Quantum Electronics and Laser Science Conference, 1993, OSA Technical Digest Series, Vol. 12 (Optical Society of America, Washington DC, 1993).
- [11] Yu. B. Ovchinnikov, J. Söding, and R. Grimm, *JETP Lett.* **61**, 21 (1995).
- [12] P. Desbiolles, M. Arndt, P. Szriftgiser, and J. Dalibard, *Phys. Rev. A* **54**, 4292 (1996).
- [13] B. T. Wolschrijn, D. Voigt, R. Jansen, R. A. Cornelussen, N. Bhattacharya, R. J. C. Spreeuw, and H. B. van Linden van den Heuvell, *Phys. Rev. A* **64**, 065403 (2001).
- [14] R. A. Cornelussen, A. H. van Amerongen, B. T. Wolschrijn, R. J. C. Spreeuw, and H. B. van Linden van den Heuvell, *Eur. Phys. J. D* **21**, 347 (2002).
- [15] H. Gauck, M. Hartl, D. Schneble, H. Schnitzler, T. Pfau, and J. Mlynek, *Phys. Rev. Lett.* **81**, 5298 (1998).
- [16] Yu. B. Ovchinnikov, I. Manek, and R. Grimm, *Phys. Rev. Lett.* **79**, 2225 (1997).
- [17] L. Cagnet, V. Savalli, G. Zs. K. Horvath, D. Holleville, R. Marani, N. Westbrook, C. I. Westbrook, and A. Aspect, *Phys. Rev. Lett.* **81**, 5044 (1998).
- [18] *Handbook of Mathematical Functions*, 9th ed., edited by M. Abramowitz and I. A. Stegun (Dover, New York, 1972).
- [19] C. Henkel, J.-Y. Courtois, R. Kaiser, C. Westbrook, and A. Aspect, *Laser Phys.* **4**, 1042 (1994).
- [20] J. Dalibard, Y. Castin, and K. Mølmer, *Phys. Rev. Lett.* **68**, 580 (1992).
- [21] K. Mølmer, Y. Castin, and J. Dalibard, *J. Opt. Soc. Am. B* **10**, 524 (1993).
- [22] M. Liebmann and B. Thaller, *Quantum Kernel* (1998) distributed with B. Thaller, *Visual Quantum Mechanics* (Springer-Verlag, New York, 2000), or available at <http://www.kfunigraz.ac.at/imawww/vqm/pages/dlschroed.html>
- [23] MATHEMATICA<sup>(R)</sup> 5 (Wolfram Research, Inc., Champaign, IL, 2003) (<http://www.wolfram.com>)
- [24] J. D. Jackson, *Classical Electrodynamics*, 3rd ed. (Wiley, New York, 1999).